Distributed Turbo Trellis Coded Modulation for Cooperative Communications

Soon Xin Ng[1], Yonghui Li[2] and Lajos Hanzo[1]
[1]School of Electronics and Computer Science, University of Southampton, SO17 1BJ, United Kingdom.
Email: {sxn,lh}@ecs.soton.ac.uk
[2]School of Electrical & Information Engineering, University of Sydney, Sydney, NSW, 2006, Australia.
Email: lyh@ee.usyd.edu.au

***Abstract*— In this contribution, we propose a Distributed Turbo Trellis Coded Modulation (DTTCM) scheme for cooperative communications. The DTTCM scheme is designed based on its decoding convergence with the aid of non-binary Extrinsic Information Transfer (EXIT) charts. The source node transmits TTCM symbols to both the relay and the destination nodes during the first transmission period. The relay performs TTCM decoding and re-encodes the information bits using a Recursive Systematic Convolutional (RSC) code regardless whether the relay can decode correctly or not. Only the parity bits are transmitted from the relay node to the destination node during the second transmission period. The resultant symbols transmitted from the source and relay nodes can be viewed as the coded symbols of a three-component parallel-concatenated TTCM scheme. At the destination node, a novel three-component TTCM decoding is performed. It is shown that the performance of the DTTCM matches exactly the EXIT chart analysis. It also performs very closely to its idealised counterpart that assumes perfect decoding at the relay.**

***Index Terms*— Cooperative Diversity, Turbo Trellis Coded Modulation.**

I. Introduction

The wireless communication systems of future generations are required to provide reliable transmissions at high data rates in order to offer a variety of multimedia services. Space time coding schemes [1], which employ multiple transmitters and receivers, are among the most efficient techniques designed for providing a high diversity gain, provided that the associated Multiple-Input Multiple-Output (MIMO) channels [2]–[4] experience independent fading. However, it is difficult to eliminate the correlation of the signals when using multiple antennas at the mobile unit due to its limited size. In order to circumvent this problem, cooperative diversity schemes were proposed in [5]–[7]. More specifically, each mobile unit collaborates with one partner or a few partners for the sake of reliably transmitting its own information and of its partners jointly, which emulates a virtual MIMO scheme. The two most popular collaborative protocols used between the source, relay and destination nodes are the Decode-And-Forward (DAF) as well as the Amplify-And-Forward (AAF) schemes. However, a strong channel code is required for mitigating the potential error propagation in the DAF scheme or the noise enhancement in the AAF scheme.

Turbo codes based on the parallel-concatenation of two binary Recursive Systematic Convolutional (RSC) codes were proposed in [8], [9] for approaching the channel capacity. Turbo Trellis Coded Modulation (TTCM) [10] is a joint coding and modulation scheme that has a structure similar to that of the family of binary turbo codes, but instead of binary RSC codes it employs two identical parallel-concatenated Trellis Coded Modulation (TCM) [11] schemes as component codes. The design of the TTCM scheme outlined in [10] was based on the search for the best component TCM codes using the so-called 'punctured' minimal distance criterion for approaching the capacity of the Additive White Gaussian Noise (AWGN) channel. Recently, various TTCM schemes were designed in [12] with the aid of Extrinsic Information Transfer (EXIT) charts [13], [14] for approaching the capacity of the Rayleigh fading channel.

The financial support of the EPSRC UK and that of the European Union under the auspices of the Optimix project is gratefully acknowledged.

Distributed turbo codes [15] have also been proposed for cooperative communications, although under the simplifying assumption of having a perfect communication link between the source and the relay nodes. It was shown in [16] that parallel-concatenated turbo codes having two or more component codes constitute 'good codes' provided that sufficiently long pseudorandom interleavers are used between the component codes. Although two component codes are sufficient for a turbo code in non-cooperative communication scenarios, we found that three-component turbo codes are more beneficial in cooperative communications. Hence in this contribution, we proposed a power and bandwidth efficient Distributed TTCM (DTTCM) scheme for cooperative communications, where our design takes into consideration the realistic condition of having an imperfect source-relay communication link. We first design a TTCM scheme employing three RSC component encoders based on its decoding convergence using EXIT charts. Then we invoke this TTCM scheme for cooperative communications, where the source employs a two-component TTCM encoder and the relay employs both a two-component TTCM decoder as well as a single RSC encoder. A form of incremental redundancy [17] is introduced by the relay node, where the parity bits at the output of the relay's RSC encoder are communicated to the destination node. At the destination, a novel three-component TTCM decoder is used. The decoding convergence of the three-component TTCM decoder depends on the specific choice of the component codes as well as on the distance between the cooperating nodes.

The paper is organised as follows. The system model is described in Section II. The novel DTTCM encoder and decoder are highlighted in Sections III and IV, respectively. The design and analysis of the proposed scheme is provided in Section V. Our simulation results are discussed in Section VI. Finally, our conclusions are offered in Section VII.

II. System Model

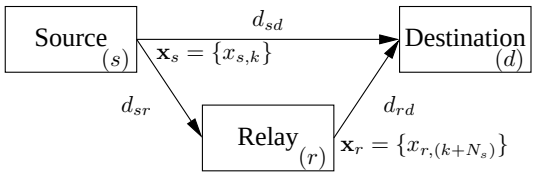

Fig. 1. Schematic of a two-hop relay-aided system, where d_{ab} is the geographical distance between node a and node b.

The schematic of a two-hop relay-aided system is shown in Fig. 1,

where the source node (s) transmits a frame of coded symbols $\mathbf{x}_s$ to the relay node (r) and the destination node (d) during the first transmission period while the relay node first decodes the information and then re-encodes it and finally transmits a frame of coded symbols $\mathbf{x}_r$ to the destination node during the second transmission period. The communication links seen in Fig. 1 are subject to both long-term free-space path loss as well as to short-term uncorrelated Rayleigh fading.

Let d_{ab} denote the geometrical distance between nodes a and b. The path loss between these nodes can be modelled by [18]:

$$P(ab) = K/d_{ab}^{\alpha} \ , \tag{1}$$

where K is a constant that depends on the environment and α is the path loss exponent. For a free-space path loss model we have $\alpha = 2$. The relationship between the energy $E(sr)$ received at the relay node and that of the destination node $E(sd)$ can be expressed as:

$$E(sr) = \frac{P(sr)}{P(sd)} E_{s,d} = G_{sr} E_{sd} \ , \tag{2}$$

where G_{sr} is the power-gain (or geometrical gain) [18] experienced by the source-to-relay link with respect to the source-to-destination link as a benefit of its reduced distance and path loss, which can be computed as:

$$G_{sr} = \left(\frac{d_{sd}}{d_{sr}}\right)^2 \ . \tag{3}$$

Similarly, the power-gain at the relay-to-destination link with respect to the source-to-destination link can be formulated as:

$$G_{rd} = \left(\frac{d_{sd}}{d_{rd}}\right)^2 \ . \tag{4}$$

Naturally, the power-gain at the source-to-destination link with respect to itself is unity, i.e. $G_{sd} = 1$.

The kth received signal at the relay node during the first transmission period, where N_s number of symbols are transmitted from the source node, can be written as:

$$y_{r,k} = \sqrt{G_{sr}} \ h_{sr,k} \ x_{s,k} + n_{r,k} \ , \tag{5}$$

where $k \in \{1, \ldots, N_s\}$ and $h_{sr,k}$ is the Rayleigh fading coefficient between the source node and the relay node at instant k, while $n_{r,k}$ is the AWGN having a variance of $N_0/2$ per dimension. By contrast, the kth received symbol at the destination node can be expressed as:

$$y_{d,k} = h_{sd,k} \ x_{s,k} + n_{d,k} \ , \tag{6}$$

where $h_{sd,k}$ is the Rayleigh fading coefficient between the source node and the destination node at instant k, while $n_{d,k}$ is the AWGN having a variance of $N_0/2$ per dimension. Similarly, the jth received symbol at the destination node during the second transmission period, where N_r number of symbols are transmitted from the relay node, is given by:

$$y_{d,j} = \sqrt{G_{rd}} \ h_{rd,j} \ x_{r,j} + n_{d,j} \ , \tag{7}$$

where $j \in \{1 + N_s, \ldots, N_r + N_s\}$ and $h_{rd,j}$ is the Rayleigh fading coefficient between the relay node and the destination node at instant j, while $n_{d,j}$ is the AWGN having a variance of $N_0/2$ per dimension.

III. DTTCM Encoder

In our DTTCM scheme, we consider an 8PSK-assisted two-component TTCM encoder at the source node as well as a QPSK-assisted RSC encoder at the relay node. Note that the relay transmits only the parity bits so that the systematic bits are transmitted only once, which is during the first transmission period. Although we can employ BPSK modulation at the relay, we found that QPSK modulation can still provide a good decoding performance at the destination node, while reducing the transmission period at the relay to half of that when employing BPSK modulation. If the relay is capable of detecting the signals received from the source node without errors during the first transmission period, then we can view the three encoders employed at both the source and relay nodes as a three-component parallel-concatenated TTCM encoder, which is depicted in Fig. 2. The notations $\mathbf{u}$, $\mathbf{x}_s$ and $\mathbf{x}_r$ used in Fig. 2 denote the sequences of the m-bit information symbols, $(m+1)$-bit modulated symbols at the source node and the 2-bit QPSK symbols at the relay node, respectively. The notations π_s and π_r in Fig. 2 denote the symbol-wise random interleaver used at the source node and relay node, respectively. We do not use code termination for simplicity, hence the length of the symbol interleavers used at both the source and relay nodes equals to N_s symbols. The puncturer denoted as Λ in Fig. 2 is used to improve the overall throughput of the scheme. We found that a good performance can be achieved by transmitting only the parity bits generated at the output of the RSC encoder at the relay node.

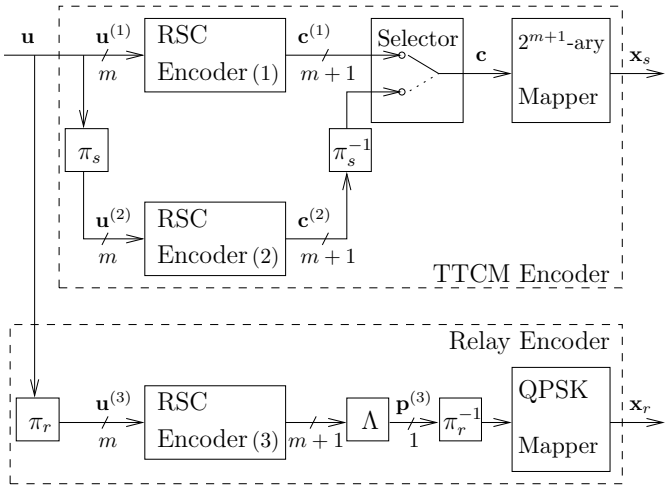

Fig. 2. The schematic of a three-component parallel-concatenated TTCM encoder. This corresponds also to the DTTCM scheme, when there are no decoding errors at the relay node.

Non-binary RSC codes having a generator polynomial of $[13\ 2\ 4]_{10}$ are used as the component codes, where the code rate is given by $R = m/(m+1) = 2/3$. The overall throughput of this two-hop cooperative scheme can be computed as:

$$\eta \ = \ \frac{N_i}{N_s + N_r} \ [\text{bps}] \ , \tag{8}$$

where N_i is the number of information bits transmitted within a duration of $(N_s + N_r)$ symbol periods. Again, N_s is the number of modulated symbols per frame from the source node and N_r is the number of modulated symbols per frame from the relay node. Since no code termination is used, we have $N_i = m\ N_s$. The conventional two-component TTCM scheme has a throughput of $\eta = m/(m+1) \times \log_2(8) = 2$ bps due to the employment of 8PSK modulation and a selector that punctures away the even-position coded symbols from the upper TTCM component encoder as well as the odd-position coded symbols from the lower TTCM component encoder. Note that the number of symbols per transmission burst at the relay node is given by $N_r = N_s/2$ due to the employment of QPSK modulation and a puncturer that removes all systematic bits. Hence, the overall effective throughput of the DTTCM scheme is given by $\eta = (m\ N_s)/(N_s + 0.5N_s) = 1.3333$ bps. The Signal

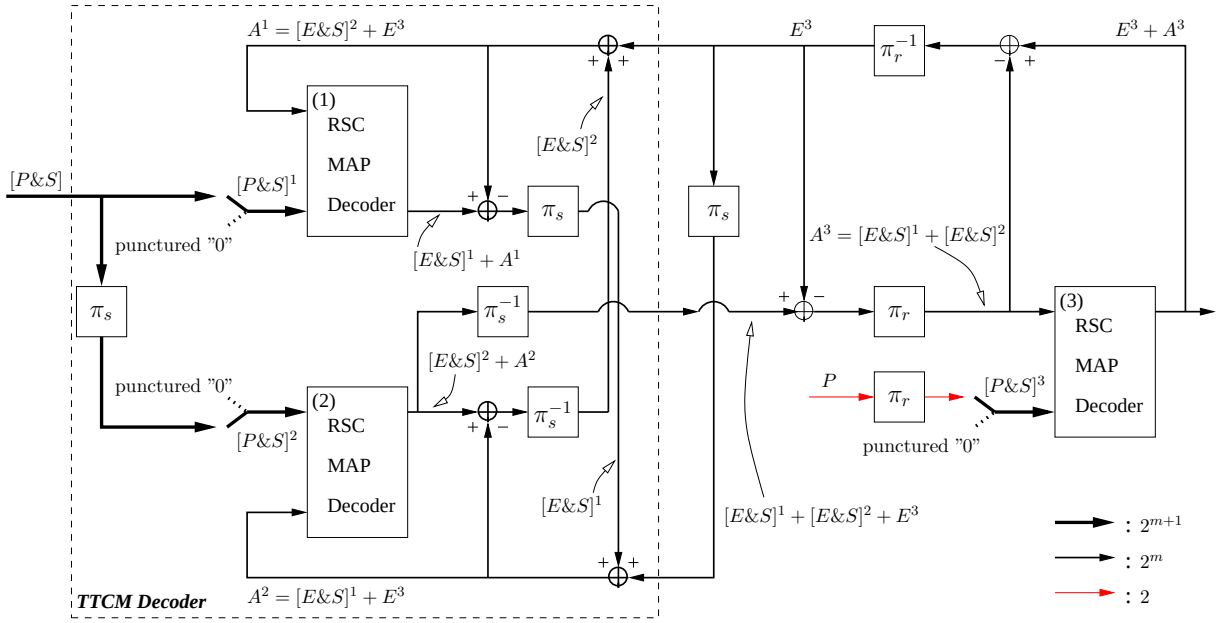

Fig. 3. The schematic of the DTTCM decoder. The input to the TTCM decoder denoted as ($[P\&S]$) is from the $M = 2^{m+1}$-ary demapper while the input to the third decoder denoted as (P) is from the QPSK demapper.

to Noise Ratio (SNR) per bit is given by $E_b/N_0 = \text{SNR}/\eta$. Hence, the DTTCM scheme suffers from a penalty of 1.76 dB in terms of E_b/N_0 due to a reduction of 0.6667 bps in the throughput, when compared to the conventional TTCM scheme.

IV. DTTCM Decoder

The novel decoder structure of the DTTCM scheme is illustrated in Fig. 3, where there are three constituent decoders, each labelled with a round-bracketed index. Symbol-based MAP algorithms [19] operating in the logarithmic-domain are employed by the RSC decoders. The notations P, S, A and E denote the logarithmic-domain probabilities of the parity information, of the systematic information, of the $a\ priori$ information and of the $extrinsic$ information, respectively. There are 2^{m+1} probabilities associated with an $(m+1)$-bit TTCM-coded symbol, which have to be determined at the soft demapper for the MAP decoder [19]. These probabilities are input to the TTCM MAP decoder as $[P\&S]$, which indicates the inseparable nature of the parity and systematic information [10], [19] within a symbol. The $a\ posteriori$ information of the m-bit systematic part of an $(m+1)$-bit TTCM symbol at the output of one of the constituent TCM decoders can be separated into two components ([19, Section 9.4] and [10]):

1) the inseparable $extrinsic$ and systematic component $[E\&S]$ also referred to as the $intrinsic$ component, which is generated by one of the constituent TCM decoders, and
2) the $a\ priori$ component A, which is provided by the other constituent TCM decoder.

However, in our proposed scheme the $a\ priori$ component A comprises also the additional $extrinsic$ information provided by the third RSC decoder, namely E^3, as we can see from Fig. 3. More explicitly, we have $A^{(1,2)} = [E\&S]^{(2,1)} + E^3$, where the extrinsic component E^3 contributing to A^2 is the symbol-interleaved version of E^3 contributing to A^1. The $a\ posteriori$ information of the m-bit systematic part of an $(m+1)$-bit TTCM symbol provided by the second TCM decoder is then symbol-deinterleaved and fed to the third RSC decoder. The inputs of the third RSC decoder are:

1) $A^3 = [E\&S]^1 + [E\&S]^2$, which is the interleaved version of the extrinsic and systematic information provided by the TTCM decoder, and
2) $[P\&S]^3$, which is the depunctured and interleaved version of the soft information provided by the QPSK demapper denoted as P in Fig. 3.

V. Design and Analysis

The first step in our design is to determine the decoding convergence of the two-component TTCM scheme at the output of the communication link between the source and the relay nodes. Non-binary EXIT charts [14] are used to visualise the input/output characteristics of the non-binary constituent RSC MAP decoders in terms of their average mutual information transfer. The *a priori* mutual information I_{A_k} is related to the *a priori* symbol probability of the kth component decoder, while the *extrinsic* mutual information I_{E_k} is related to the *extrinsic* symbol probability of the kth component decoder [14].

The EXIT chart of the two-component TTCM-8PSK scheme recorded for the classic non-cooperative scenario is depicted in Fig. 4, where the decoding trajectory is computed based on a frame length of 10 000 symbols. When there is no path loss, the receive SNR equals the transmit SNR. As we can see from Fig. 4, a receive SNR of about 9.0 dB is needed in order to attain a decoding convergence, since at 8.5 dB the EXIT-tunnel remains closed. Fig. 4 also corresponds to the performance of the TTCM-8PSK scheme for the source-to-relay link. The receive SNR can be computed as:

$$\text{SNR}_r = \text{SNR}_t + 10\log_{10}(G_{sr})\ [\text{dB}]\ , \tag{9}$$

where SNR_t is the transmit SNR and G_{sr} was defined in (3). Hence, a receive SNR of 9.0 dB can be achieved by various combinations of SNR_t and G_{sr}. For example, we have $\text{SNR}_r = 9.0$ dB for $\text{SNR}_t = 3.0$ dB and for a power-gain of $G_{sr} = 4$ as well as for $\text{SNR}_t = 0.0$ dB and $G_{sr} = 8$. Hence, depending on G_{sr}, which is related to the distance between the source, relay and destination nodes in (3), we can determine the minimum required transmit SNR at the source node in order to minimise the probability of decoding errors at the relay node.

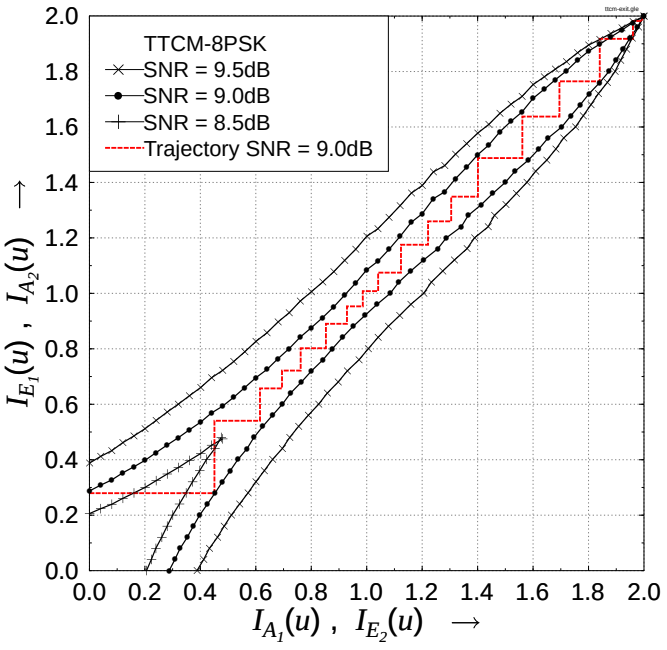

Fig. 4. The EXIT curves of the TTCM-8PSK scheme for non-cooperative scenario. This corresponds also to the TTCM-8PSK performance at the source-to-relay link where the SNR shown is the receiver SNR which is related to the transmit SNR and the geometrical gain G_{sr}.

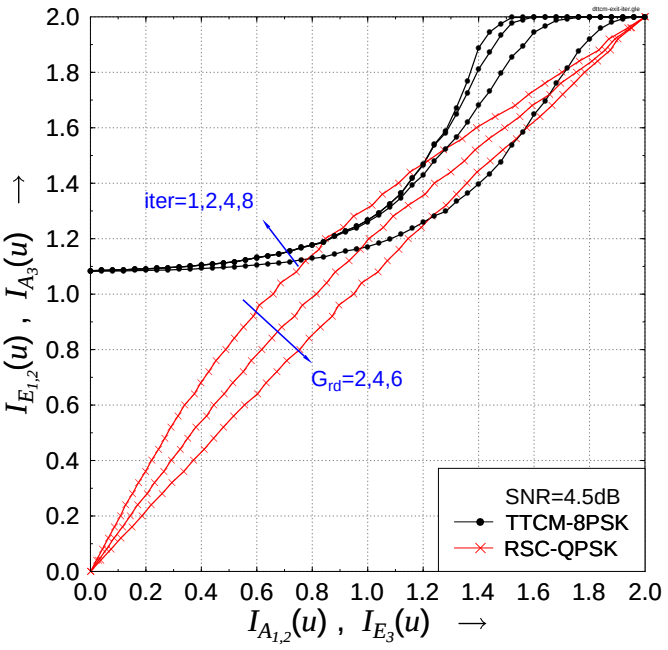

Fig. 5. The EXIT curves of the DTTCM scheme for a transmit SNR of 4.5 dB at both the source and the relay nodes. The EXIT curves of the TTCM-8PSK decoder employing different number of inner iterations are shown. The EXIT curves of the RSC-QPSK decoder recorded for various relay-to-destination power-gains are given.

The second step in our design is to analyse the decoding convergence of the three-component TTCM decoder at the destination node. The EXIT curves of the TTCM-8PSK decoder employing various number of inner iterations and the RSC-QPSK decoder plotted for various relay-to-destination power-gains are shown in Fig. 5. We assume perfectly error-free DAF relaying in our EXIT chart analysis, where the relay is capable of detecting the signals arriving from the source node without error. We refer to the DTTCM arrangement benefitting from perfect DAF relaying as the DTTCM-perfect scheme. As we can see from Fig. 5, having more than 2 TTCM iterations yields a diminishing advantage. The various values of the relay-to-destination power-gain G_{sr} can be obtained by changing the location of the relay nodes appropriately. Observe that an open tunnel emerges in the EXIT chart of Fig. 5, when the TTCM-8PSK decoder employs two inner iterations and we have $G_{rd} = 4$, which corresponds to $d_{rd} = d_{sd}/2$.

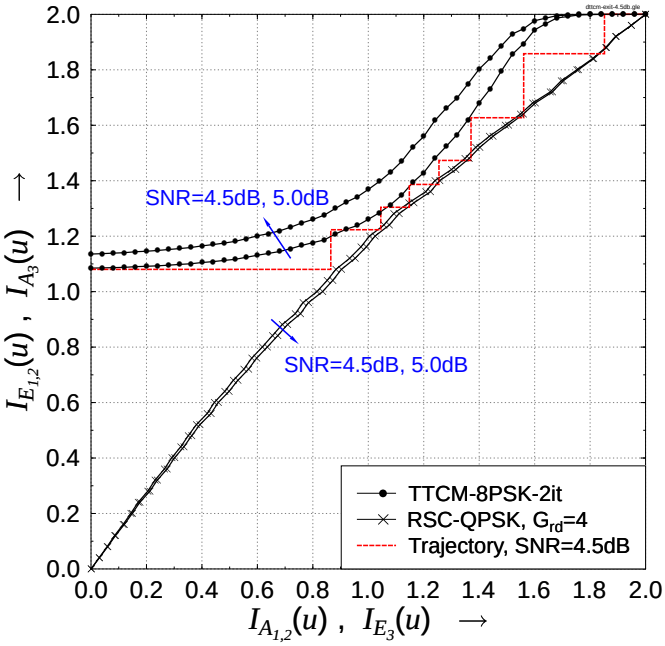

Fig. 6. The EXIT curves of the DTTCM scheme for a transmit SNR of 4.5 dB and 5.0 dB at both the source and the relay nodes.

The third step in our design is to verify our prediction by computing the corresponding Monte-Carlo simulation-related decoding trajectory, for the DTTCM-perfect scheme. The decoding trajectory based on a frame length of $N_s = 10\ 000$ is shown in Fig. 6 for a transmit SNR of 4.5 dB.

VI. Results and Discussions

The final step in our analysis is to compare the achievable performance of the DTTCM scheme employing a realistic relay node, which potentially induces error propagation, to that of the DTTCM-perfect scheme. The Bit Error Ratio (BER) versus transmit SNR performance of the DTTCM and TTCM schemes is shown in Fig. 7. The number of TTCM decoding iterations was fixed to $I^r = 8$ at the relay node of the DTTCM scheme. At the destination node, the number of 'inner' TTCM decoding iterations was fixed to $I_i^d = 2$, while the number of 'outer' decoding iterations between the TTCM decoder and the RSC decoder at the destination was fixed to $I_o^d = 8$. Hence, the first and second RSC decoders of the TTCM scheme are activated $I = I_i^d \times I_o^d = 16$ times each, while the third RSC decoder is activated $I_o^d = 8$ times in our simulation. We assume that both the

source and relay nodes transmit their signals using the same transmit energy, hence the same transmit SNR.

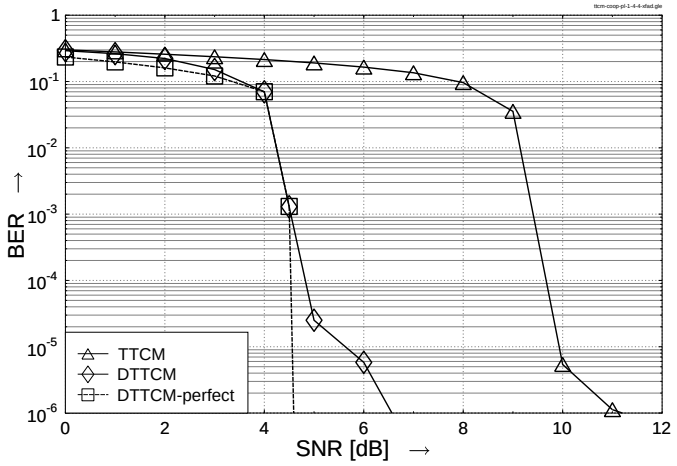

Fig. 7. BER versus transmit SNR performance of the DTTCM and TTCM schemes for a frame length of $N_s = 10\,000$ symbols. The relay node of the DTTCM is placed half-way between the source and relay nodes, i.e. $G_{sr} = G_{rd} = 4$.

As seen in Fig. 7, the performance of the DTTCM-perfect scheme matches the EXIT chart prediction illustrated in Fig. 6, while the DTTCM scheme performs similarly to the DTTCM-perfect scheme. At a BER of 10^{-4}, the DTTCM arrangement outperforms the TTCM scheme by approximately 4.84 dB in terms of the required transmit SNR, which corresponds to $4.84 - 1.76 = 3.08$ dB in terms of E_b/N_0. In fact at a transmit SNR of 5 dB we have a receive SNR of $5 + 10\log_{10}(G_{sr}) = 11$ dB at the relay node for $G_{sr} = 4$. As we can see from Fig. 7 the non-cooperative TTCM scheme, which employs 8 TTCM decoding iterations, has a BER of approximately 10^{-6} at SNR $= 11$ dB. This implies that at a transmit SNR of 5 dB, the relay would suffer from a BER of approximately 10^{-6}. These decoding errors propagate to the destination node causing a BER of approximately 2.5×10^{-5} at a transmit SNR of 5 dB as shown in Fig. 7. Hence, when the BER at the relay node is very low, it would not cause too much BER degradation at the destination. The imperfect relay signals would help the DTTCM decoder at the destination to perform well when the BER at the relay node is very low.

Note furthermore that at $G_{sr} = 4$ and at a transmit SNR of 4.5 dB the receive SNR at the relay node becomes 10.5 dB, which is $10.5 - 9.0 = 1.5$ dB higher than the TTCM decoding threshold of 9.0 dB, as shown in Fig. 4. Hence, the DTTCM scheme's performance can be further improved by moving the relay node farther away from the source node and hence closer to the destination node, until the receive SNR at the relay node is just above 9.0 dB. This would result in a higher G_{rd} value and hence a higher receive SNR at the destination node during the second transmission period.

VII. Conclusion

A power and bandwidth efficient DTTCM scheme was proposed for cooperative communications based on the three-component TTCM design of Fig. 3. A two-component TTCM scheme is required at the source node of Fig. 1 in order to minimise the decoding error probability at the relay node using the minimum possible transmit SNR. Once the received SNR at the relay node exceeds the decoding threshold, the TTCM decoder at the relay node becomes capable of reliably decoding the source signals. The relay node employs a simple RSC encoder and only its parity bits are transmitted to the destination node for providing incremental redundancy. The EXIT chart of the three-component TTCM decoder seen in Fig. 5 reveals that a beneficial combination of the transmit SNR and the relay location results in a decoding convergence at a lower SNR than the classic TTCM scheme. Our simulation results seen in Fig. 7 show that the DTTCM outperforms the conventional non-cooperative TTCM scheme by 3.08 dB at a BER of 10^{-4}, when the relay is located half-way between the source and destination nodes.

References

[1] V. Tarokh, N. Seshadri, and A. R. Calderbank, "Space-time codes for high data rate wireless communication: Performance criterion and code construction," *IEEE Transactions on Information Theory*, vol. 44, pp. 744–765, March 1998.

[2] G. Foschini Jr. and M. Gans, "On limits of wireless communication in a fading environment when using multiple antennas," *Wireless Personal Communications*, vol. 6, pp. 311–335, March 1998.

[3] E. Telatar, "Capacity of multi-antenna Gaussian channels," *European Transactions on Telecommunication*, vol. 10, pp. 585–595, Nov–Dec 1999.

[4] S. X. Ng and Hanzo, "On the MIMO Channel Capacity of Multi-Dimensional Signal Sets," *IEEE Transactions on Vehicular Technology*, vol. 55, pp. 528–536, March 2006.

[5] A. Sendonaris, E. Erkip and B. Aazhang, "User cooperation diversity part I: System description," *IEEE Transactions on Communications*, vol. 51(11), pp. 1927–1938, 2003.

[6] N. Laneman, D. N. C. Tse and G. W. Wornell, "Cooperative diversity in wireless networks: efficient protocols and outage behavior," *IEEE Trans. on Information Theory*, vol. 50, no. 12, pp. 3062–3080, 2004.

[7] E. Zimmermann, P. Herhold and G. Fettweis, "On the performance of cooperative relaying protocols in wireless networks," *European Transactions on Telecommunications*, vol. 16, no. 1, pp. 5–16, 2005.

[8] C. Berrou and A. Glavieux and P. Thitimajshima, "Near Shannon limit error-correcting coding and decoding: Turbo codes," in *Proceedings of the International Conference on Communications*, (Geneva, Switzerland), pp. 1064–1070, May 1993.

[9] S. Benedetto and G. Montorsi, "Design of parallel concatenated convolutional codes," *IEEE Transactions on Communications*, vol. 44, pp. 591–600, May 1996.

[10] P. Robertson and T. Wörz, "Bandwidth-efficient turbo trellis-coded modulation using punctured component codes," *IEEE Journal on Selected Areas in Communications*, vol. 16, pp. 206–218, Feb 1998.

[11] G. Ungerböck, "Channel coding with multilevel/phase signals," *IEEE Transactions on Information Theory*, vol. IT-28, pp. 55–67, January 1982.

[12] S. X. Ng, J. Kliewer, O. R. Alamri and L. Hanzo, "On the design of Turbo Trellis Coded Modulation schemes using symbol-based EXIT charts," in *IEEE Vehicular Technology Conference (Fall)*, (Montreal, Canada), pp. 1–5, September 2006.

[13] S. ten Brink, "Convergence behaviour of iteratively decoded parallel concatenated codes," *IEEE Transactions on Communications*, vol. 49, pp. 1727–1737, October 2001.

[14] J. Kliewer, S. X. Ng, and L. Hanzo, "Efficient computation of EXIT functions for non-binary iterative decoding," *IEEE Transactions on Communications*, vol. 54, pp. 2133–2136, December 2006.

[15] B. Zhao and M. C. Valenti, "Distributed turbo coded diversity for relay channel," *IEE Electronics Letters*, vol. 39, pp. 786–787, May 2003.

[16] H. Jin and R. J. McEliece, "Coding theorems for turbo code ensembles," *IEEE Transactions on Information Theory*, vol. 48, pp. 1451–1461, June 2002.

[17] R. Liu, P. Spasojevic and E. Soljanin, "Incremental redundancy cooperative coding for wireless networks: Cooperative diversity, coding and transmission energy gains," *IEEE Transactions on Information Theory*, vol. 54, pp. 1207–1224, March 2008.

[18] H, Ochiai, P. Mitran and V. Tarokh, "Design and analysis of collaborative diversity protocols for wireless sensor networks," in *Proceedings of IEEE VTC Fall*, (Los Angeles, USA), pp. 4645 – 4649, 26-29 September 2004.

[19] L. Hanzo, T.H. Liew and B.L. Yeap, *Turbo Coding, Turbo Equalisation and Space Time Coding for Transmission over Wireless channels*. New York, USA: John Wiley IEEE Press, 2002.